Numerical Schemes Applicable in Contaminant Hydrology Calculations

by
Hillel Rubin*

Kansas Geological Survey Open-File Report 94-7

*On leave from the Department of Civil Engineering, Technion—Israel Institute of Technology, Haifa 32000, Israel.

List of Figures

Abstract

This report concerns the development and use of various types of finite difference numerical schemes for the simulation of basic cases of aquifer contamination. The contaminant concentration is prescribed at the aquifer boundary or the penetrating contaminant flux is prescribed at that boundary. The study addresses to a hierarchy of possible approximate approaches that can be useful in some classes of contaminant hydrology problems. The aquifer is represented by a simplified conceptual model allowing very basic simplifications and tests of the numerical schemes. The numerical schemes developed in this study, can easily be modified and extended to cases that are more complicated than those considered in the present study.

Notation

a	dimensionless transverse dispersivity
a_L	dimensionless longitudinal dispersivity
A	coefficient defined in eqs. (52) and (53)
BL	boundary layer
C	normalized contaminant concentration
C_b	normalized concentration at the boundary of the domain
C_T	normalized concentration at the top of the BL
C^*	contaminant concentration [ML^{-3}]
C_0	concentration of reference [ML^{-3}]
CBL	classical BL
d	representation of δ in figures
$\tilde{D}$	dispersion tensor [L^2T-1]
D_x	longitudinal dispersion coefficient [L^2T-1]
D_y	transverse dispersion coefficient [L^2T-1]
g	gravitational acceleration [LT^{-2}]
h	dummy variable representing Δx or Δy
i	$\sqrt{-1}$
k	permeability [L^2]
l_0	length scale [L]
L	power series
m	number of time step
n	power coefficient
(n)	number of iteration
p	pressure [$ML^{-1}T^{-2}$]
q	specific discharge of groundwater [LT^{-1}]
q_m	mass flux of the contaminant penetrating into the aquifer [$ML^{-2}T^{-1}$]

q_R	relative penetrating mass flux
r	number of the nodal point in the longitudinal direction
ROI	region of interest
s	number of the nodal point in the vertical direction
t	dimensionless time
t^*	time [T]
t_0	time scale [T]
TSBL	top specified BL
u	unit step function
V	interstitial flow velocity [LT^{-1}]
x	dimensionless longitudinal coordinate
x_{max}	length of the domain
x_b	starting point for the development of the ROI
x^*	longitudinal coordinate [L]
y	dimensionless vertical coordinate
y^*	vertical coordinate [L]
$\alpha_0, \alpha_1, \alpha_2, \alpha_3...$	coefficients defined in eq. (28)
β	dummy coefficient representing β_1 or β_2
β_1	coefficient of oscillations in the x direction
β_2	coefficient of oscillations in the y direction
γ	coefficient of growth with time
δ	thickness of the ROI
δ_0	value of y at which concentration is negligible
Δt	time step
Δx	longitudinal interval
Δy	vertical interval
η	dimensionless coordinate of the BL

η_T	value of η at $y = \delta$
θ	dimensionless coordinate defined in eq. (22)
μ	fluid viscosity
ξ	coefficient of amplification
ρ	fluid density [ML^{-3}]
ϕ	porosity
ω	coefficient of over-relaxation

Introduction

This study addresses to the development of approximate methods for the simulation of groundwater contamination. We refer to a very simplified conceptual model of an aquifer subject to contamination as shown in fig. 1(a). The aquifer is unconfined, and saturated thickness is great enough so that the Dupuit approximation can be useful. Flow direction and streamlines are almost horizontal. The longitudinal x^* axis represents the surface through which contaminants are introduced into the aquifer. The y^* axis is vertical in the downward direction.

Flow conditions and contaminant transport in the domain of fig. 1(a) are governed by the following differential equations

$$\vec{q} = -\frac{k}{\mu}(\nabla p - \rho \vec{g}) \tag{1}$$

$$\frac{\partial C^*}{\partial t^*} + \vec{V} \cdot \nabla C^* = \nabla \cdot \left(\tilde{D} \nabla C^* \right) \tag{2}$$

where, q is the specific discharge; k is the permeability; μ is the fluid viscosity; p is the pressure; ρ is the fluid density; g is the gravitational acceleration; C^* is the contaminant concentration; V is the interstitial flow velocity; $\tilde{D}$ is the dispersion tensor; and t^* is the time.

The system of partial differential eqs. (1) and (2) can be solved by various types of numerical procedures. However, the Dupuit approximation is usually employed for the solution of eq. (1). In the particular simplified domain shown in fig. 1(a), this approximation yields a uniform horizontal flow velocity, provided that the permeability is uniform. Then eq. (2) is represented as

$$\frac{\partial C^*}{\partial t^*} + V \frac{\partial C^*}{\partial x^*} = D_x \frac{\partial^2 C^*}{\partial x^{*2}} + D_y \frac{\partial^2 C^*}{\partial y^{*2}} \tag{3}$$

where x^* and y^* are the longitudinal and vertical coordinates, respectively; D_x and D_y are the longitudinal and transverse dispersion coefficients, respectively.

As the domain is homogeneous and isotropic we may refer to the following characteristics of the domain

$$l_0,\ t_0 = l_0 / V,\ C_0 \tag{4}$$

where l_0 is an adopted unit length along the surface $y^* = 0$; t_0 is the time corresponding to l_0 for the velocity V; C_0 is a concentration of reference. The value of C_0 should somehow be connected with prescribed boundary values or risk values of the contaminant concentration.

The characteristics of eq. (4) are used to nondimensionalize the variables of eq. (3) as

$$x = x^*/l_0;\ \ y = y^*/l_0;\ \ t = t^*/t_0;\ \ C = C/C_0 \tag{5}$$

Introducing these terms into eq. (3), we obtain

$$\frac{\partial C}{\partial t} + \frac{\partial C}{\partial x} = a_L \frac{\partial^2 C}{\partial x^2} + a\frac{\partial^2 C}{\partial y^2} \tag{6}$$

where, a_L and a are the dimensionless longitudinal and transverse dispersivities which are defined as

$$a_L = D_x/(l_0 V);\ \ a = D_y/(l_0 V) \tag{7}$$

The following sections of this report are devoted to the development of numerical solutions to eq. (6) subject to appropriate initial and boundary conditions relevant to cases of groundwater contamination in aquifers that can approximately be described by the conceptual model of fig. 1(a).

If at the boundary $y^* = 0$ the value of the contaminant concentration is prescribed, then it seems reasonable to adopt

$$C_0 = C^*(x^*, 0, t^*) \tag{8}$$

namely contaminant concentrations are normalized with regard to the concentration at the x^* axis. Under such conditions eq. (6) is subject to the following initial and boundary conditions

$$\begin{aligned} &C = C(x,y,t) \qquad x,y,t \geq 0 \\ &C(x,y,0) = 0 \qquad \textit{except for } C(x,0,0) = 1.0 \\ &C(x,0,t) = 1 \\ &C(x,\infty,t) = 0 \\ &\frac{\partial C}{\partial x} \to 0 \ \textit{ at } \ x \to \infty \end{aligned} \tag{9}$$

In figure 1(b) the dimensionless domain and quantities are shown for the prescribed contaminant concentration at $y = 0$. Some of these quantities will be defined in following sections of this report.

If at the boundary $y = 0$ is prescribed, the contaminant mass flux which penetrates into groundwater, then

$$\phi D_y \frac{\partial C^*}{\partial y^*} = -q_m \quad at \quad y^* = 0 \tag{10}$$

where, q_m is the contaminant mass flux penetrating into the domain through the x^* axis; and ϕ is the porosity of the porous medium.

By introducing the normalized quantities of eqs. (5) and (7) into eq. (10) we obtain

$$a\frac{\partial C}{\partial y} = -q_R \quad at \quad y = 0 \tag{11}$$

where, q_R is the normalized flux of the penetrating contaminant

$$q_R = \frac{q_m}{qC_0} \tag{12}$$

where, q is the specific discharge of the groundwater flow.

The following initial and boundary conditions are applicable when the contaminant mass flux is prescribed at $y = 0$

$$\begin{aligned} &C = C(x,y,t) \qquad x,y,t \geq 0 \\ &C(x,y,0) = 0 \\ &\frac{\partial C}{\partial y} = -\frac{q_R}{a} \quad at \quad y = 0 \\ &C(0,y,t) = 0 \\ &C(x,\infty,t) = 0 \\ &\frac{\partial C}{\partial x} \to 0 \quad at \quad x \to \infty \end{aligned} \tag{13}$$

In fig. 1(c) the dimensionless domain and quantities are shown for the prescribed contaminant flux penetrating into groundwater at $y = 0$.

Direct Solution of the Contaminant Transport Equation

We consider some finite difference numerical schemes which can be applied to the solution of eq. (6) subject to either the boundary conditions of eq. (9) or those of eq.(13). We have chosen to apply finite difference schemes as with such schemes it is convenient to follow the various difficulties involved in the numerical simulation and to consider the use of some further approximation which are presented in following sections.

The numerical schemes developed for the solution of eq. (6) should be based on the following basic considerations: convergence, stability and accuracy.

The boundary and initial conditions of eqs. (9) and (13) indicate that when the numerical simulation starts all terms of eq. (6) have vanishing values. As long as both terms of the right-hand side of eq. (6) are very small, that equation is approximately a first order hyperbolic equation in the x, y plane. If the second term of the left-hand side is small then eq. (6) is approximately a parabolic equation in the x, t and y, t planes. If steady state conditions are established in the domain, then the first term of eq. (6) vanishes. Under such conditions eq. (6) is converted to an elliptic partial differential equation. However, if in steady state the first right-hand side term of eq. (6) is much smaller than the last term of eq.(6) then this equation is converted to a parabolic equation in the x, y plane.

In following paragraphs we consider the use of various types of numerical schemes. For every adopted scheme criteria of stability and performance will be evaluated. As long as steady state conditions are not established in the domain, we need a numerical scheme that takes into account the possible nature of eq. (6) as a first order hyperbolic equation in the x, t plane or a parabolic equation in the x, t and y, t planes. Because of the possible parabolic feature of eq. (6) it is reasonable to adopt a forward finite difference approximation with regard to the time step. In order to obtain a stable hyperbolic system we may adopt central or backward stable finite difference schemes with regard to the second left-hand side term of eq. (6). Explicit finite difference schemes can be adopted provided that the following condition is satisfied (e.g. Lapidus and Pinder, 1982)

$$\frac{\Delta t}{\Delta x} \le 1 \tag{14}$$

Implicit schemes are not subject to such a limitation. The central finite difference approximation has a smaller truncation error. The combination of either central or backward space finite differences with the forward time difference are subject to a certain amount of numerical dispersion. Choice of the central space difference for the second term of eq. (6) leads to an implicit scheme. Choice of backward space difference for that term may lead to explicit schemes as

$$\frac{C_{r,s}^{m+1} - C_{r,s}^{m}}{\Delta t} + \frac{C_{r,s}^{m+1} - C_{r-1,s}^{m+1}}{\Delta x} = a_L \frac{C_{r+1,s}^{m} - 2C_{r,s}^{m} + C_{r-1,s}^{m}}{(\Delta x)^2} + a \frac{C_{r,s+1}^{m} - 2C_{r,s}^{m} + C_{r,s-1}^{m}}{(\Delta y)^2} \tag{15}$$

$$\frac{C_{r,s}^{m+1} - C_{r,s}^{m}}{\Delta t} + \frac{C_{r,s}^{m+1} - C_{r-1,s}^{m+1}}{\Delta x} = a_L \frac{C_{r+1,s}^{m} - 2C_{r,s}^{m} + C_{r-1,s}^{m}}{(\Delta x)^2} + a \frac{C_{r-1,s+1}^{m} - 2C_{r-1,s}^{m} + C_{r-1,s-1}^{m}}{(\Delta y)^2} \tag{16}$$

where *m* is a superscript representing the time step; *r* is a subscript representing the longitudinal nodal point number, and *s* is a subscript representing the transverse (vertical) nodal point number.

Equation (15) yields the explicit numerical scheme

$$\begin{aligned} C_{r,s}^{m+1}\left(1 + \frac{\Delta t}{\Delta x}\right) = C_{r,s}^{m} + \frac{\Delta t}{\Delta x} C_{r-1,s}^{m+1} + \frac{a_L \Delta t}{(\Delta x)^2}\left(C_{r+1,s}^{m} - 2C_{r,s}^{m} + C_{r-1,s}^{m}\right) \\ + \frac{a\Delta t}{(\Delta y)^2}\left(C_{r,s+1}^{m} - 2C_{r,s}^{m} + C_{r,s-1}^{m}\right) \end{aligned} \tag{17}$$

As shown in the Appendix, the numerical scheme of eq. (17) is stable provided that the following criteria are satisfied

$$\begin{aligned} \frac{2a_L \Delta t}{(\Delta x)^2} + \frac{2a\Delta t}{(\Delta y)^2} \le 1 + \frac{\Delta t}{\Delta x} \\ \frac{2a\Delta t}{(\Delta y)^2} \le 1 \end{aligned} \tag{18}$$

Equation (16) yields the following explicit numerical scheme

$$\begin{aligned} C_{r,s}^{m+1}\left(1 + \frac{\Delta t}{\Delta x}\right) = C_{r,s}^{m} + \frac{\Delta t}{\Delta x} C_{r-1,s}^{m+1} + \frac{a_L \Delta t}{(\Delta x)^2}\left(C_{r+1,s}^{m} - 2C_{r,s}^{m} + C_{r-1,s}^{m}\right) \\ + \frac{a\Delta t}{(\Delta y)^2}\left(C_{r-1,s+1}^{m} - 2C_{r-1,s}^{m} + C_{r-1,s-1}^{m}\right) \end{aligned} \tag{19}$$

As shown in the Appendix, the numerical scheme of eq. (19) is stable provided that the following criteria are satisfied

$$\frac{2a_L\Delta t}{(\Delta y)^2}-\frac{2a_L}{\Delta x}\le 1;$$
$$\frac{2a_L\Delta t}{(\Delta x)^2}-\frac{2a\Delta t}{(\Delta y)^2}\le 1+\frac{\Delta t}{\Delta x}$$
$$\frac{2a\Delta t}{(\Delta y)^2}\le 1 \tag{20}$$

Complying with the last boundary condition of eqs. (9) and (13) we consider that $\partial C/\partial x$ for the last longitudinal nodal point and the preceding nodal point are identical.

In fig. 2 we compare simulation results obtained by use of eq. (17) with those obtained by use of eq. (19). The parameter δ, appearing in fig. 2, is defined as the value of y at which $C = 0.01$. This figure refers to the initial and boundary conditions of eq. (9), and $C = 1$ at $y = 0$. If the point identified by $C = 0.01$ is located between two adjacent vertical nodal points y_S and y_{S+1} in which $C = C_S$ and C_{S+1}, respectively, we apply a power series expansion in order to identify the value of δ. We consider that in the interval Δy between y_S and y_{S+1} the concentration is given as

$$C=(C_s-C_{s+1})L(\theta)+C_{s+1} \tag{21}$$

where

$$\theta=(y-y_s)/\Delta y \tag{22}$$

We consider

$$L(\theta)=(1-\theta)^n \tag{23}$$

where n is a power coefficient.

Introducing eq. (23) into eq. (21) and considering that $C = C_S$ at y_S we obtain

$$\delta=y_s+\Delta y\left[1-\left(\frac{0.01-C_{s+1}}{C_s-C_{s+1}}\right)^{\frac{1}{n}}\right] \tag{24}$$

Because Δy is a small interval we apply $n = 2$ in all our simulations using eq. (24).

Figure 2 shows that values of δ obtained by use of eq. (17) are larger by about 1.5 percent than those of eq. (19). Such differences are negligible when practical use is considered.

When steady state conditions are established in the domain, we may consider

$$C_{r,s}^{m+1} = C_{r,s}^{m} = C_{r,s} \tag{25}$$

By introducing eq. (25) into eq. (17) we obtain

$$C_{r,s}\left[1+\frac{2a_L}{\Delta x}+\frac{2a\Delta x}{(\Delta y)^2}\right] = C_{r-1,s}\left[1+\frac{a_L}{\Delta x}\right]+\frac{a_L}{\Delta x}C_{r+1,s}+\frac{a\Delta x}{(\Delta y)^2}C_{r,s-1}+\frac{a\Delta x}{(\Delta y)^2}C_{r,s+1} \tag{26}$$

Basically when steady state conditions are established, eq. (6) becomes an elliptic partial differential equation in the x, y plane. Eq. (26) indicates that each nodal point (r, s) in the domain is associated with five unknown values of C in (r, s) and surrounding nodal points. The constant coefficient multiplying $C_{r,\,s}$, in the equation associated with the point (r, s), is the dominant factor. Therefore, the solution of the set of linear equations represented by eq. (26) can efficiently be obtained by the successive over-relaxation (SOR) method.

The iterative procedure is given by

$$C_{r,s}^{(n+1)} = (1-\omega)C_{r,s}^{(n)} + \omega\left[\alpha_1 C_{r-1,s}^{(n+1)} + \alpha_2 C_{r+1,s}^{(n)} + \alpha_3\left(C_{r,s-1}^{(n+1)} + C_{r,s+1}^{(n)}\right)\right] \tag{27}$$

where

$$\begin{aligned} &\alpha_0 = 1+2\frac{a_L}{\Delta x}+\frac{2a\Delta x}{(\Delta y)^2};\ \alpha_1 = \left(1+\frac{a_L}{\Delta x}\right)/\alpha_0 \\ &\alpha_2 = \left(\frac{a_L}{\Delta x}\right)/\alpha_0;\ \alpha_3 = \left[\frac{a\Delta x}{(\Delta y)^2}\right]/\alpha_0 \end{aligned} \tag{28}$$

In eq. (27), (n) is the number of the iteration; ω is the over-relaxation coefficient.

In fig. 3 steady state values of δ obtained by employing the numerical scheme of eq. (27) and boundary conditions of eq. (9) are compared with values of δ obtained by use of eqs. (17) and (19) for very long simulation time of $t = 100$. All results, obtained by the various types of numerical schemes, are practically identical.

Results shown in figs. 2 and 3 indicate that in an approximate time period $t \approx 2x_{max}$ the build-up of the region of interest (ROI) is completed. Where x_{max} is the horizontal extent of the domain, and the ROI is defined as the region in which $C \geq 0.01$. Due to the introduction of the dimensionless coordinates of eq. (5), x_{max} also represents the dimensionless time period needed

for the advection of a fluid particle along the whole horizontal extent of the domain. Therefore, results of fig. 3 provide some time scale with regard to the contamination process.

Figure 4 exemplifies the application of the numerical scheme of eq. (17) in conjunction with the boundary conditions of eq. (13) to evaluate the contamination process and build-up of the ROI when the contaminant flux is prescribed at $y = 0$. It seems that the build-up time period of the ROI is not affected by the type of boundary condition of the domain shown in fig. 1.

Neglect of Longitudinal Dispersion

In the domain of fig. 1 contaminant transport in the longitudinal x direction is dominated by advection. Therefore, numerical experiments with the complete neglect of the first right-hand side term of eq. (6) are also performed in the framework of this study.

If effects of longitudinal dispersion are negligible then eq. (6) collapses to

$$\frac{\partial C}{\partial t} + \frac{\partial C}{\partial x} = a\frac{\partial^2 C}{\partial y^2} \tag{29}$$

It is convenient to evaluate the applicability of eq. (29) by referring to the establishment of steady state conditions in the domain. When steady state conditions are established eq. (29) collapses to

$$\frac{\partial C}{\partial x} = a\frac{\partial^2 C}{\partial y^2} \tag{30}$$

Equation (30) is analogous to the typical diffusion or heat conduction equation in one dimensional domain. Eq. (30) is a parabolic differential equation in the x, y domain. By the employment of the relevant boundary conditions of eq. (9), the solution of eq. (30) is (Carslaw and Jaeger, 1959)

$$C = erfc\left[y/(4ax)^{0.5}\right] \tag{31}$$

where *erfc* is the complementary error function.

By the employment of the relevant boundary conditions of eq. (13), the solution of eq. (30) is (Carslaw and Jaeger, 1959)

$$C = \frac{q_R}{a}\left[2\sqrt{\frac{ax}{\pi}}\exp\left(\frac{-y^2}{4ax}\right) - y\ erfc\left(\frac{y}{2\sqrt{ax}}\right)\right] \tag{32}$$

In figs. 5(a) and 5(b) we compare values of δ obtained by the employment of eq. (27) subject to the boundary conditions of eq. (9) with results obtained by use of eq. (31). The major objective of figs. 5(a) and 5(b) is to demonstrate the possible effect of the longitudinal dispersion on the build-up of the ROI. Therefore, figs. 5(a) and 5(b) represent two different kinds of numerical experiments. In the calculations represented by fig. 5(a) we keep $a_L = 5$ for all values of a. In all the simulations, values of δ obtained by use of eq. (27) are larger than those obtained by use of eq. (31). However, differences between values of δ calculated by use of the two different equations are not significant. Values of δ obtained in fig. 5(a) for $a = 0.05$ and $a_L = 5$, namely $a_L = 100 \cdot a$, are not much different from those obtained in fig 5(b) for $a = 0.05$ and $a_L = 0.5$, namely $a_L = 10 \cdot a$.

Figure 6 shows steady state concentration profiles obtained by use of eq. (27) subject to the boundary conditions of eq. (9) and those obtained by use of eq. (31). Differences between the two types of solution are very minor. Similar conclusion is arrived when employing eq. (27) subject to the boundary conditions of eq. (13) and eq. (32).

The numerical solutions of eq. (30) are well documented in various types of diffusion and heat conduction. However, under unsteady state conditions the simplified versions of the numerical schemes given by eqs. (17) and (19) can be applied. Since the order of the x derivatives is one, the last artificial boundary condition of eqs. (9) and (13), which refers to $x \to \infty$, can be ignored.

The simplified version of eq. (17) is

$$C_{r,s}^{m+1}\left(1+\frac{\Delta t}{\Delta x}\right)=C_{r,s}^{m}+\frac{\Delta t}{\Delta x}C_{r-1,s}^{m+1}+\frac{a\Delta t}{(\Delta y)^2}\left(C_{r,s+1}^{m}-2C_{r,s}^{m}+C_{r,s+1}^{m}\right) \tag{33}$$

The stability criterion for this numerical scheme, as shown in the Appendix, is

$$\frac{2a\Delta t}{(\Delta y)^2}\le 1 \tag{34}$$

When steady state conditions are established we apply the relationship of eq. (25) to obtain from eq. (33)

$$-\frac{a\Delta x}{(\Delta y)^2}C_{r,s-1}+\left[1+\frac{2a\Delta x}{(\Delta y)^2}\right]C_{r,s}-\frac{a\Delta x}{(\Delta y)^2}C_{r,s+1}=C_{r-1,s} \tag{35}$$

Eq. (35) represents the implicit numerical scheme for the solution of the parabolic differential equations given by eq. (30). This scheme is unconditionally stable.

The simplified version of eq. (19) is given as

$$C_{r,s}^{m+1}\left(1+\frac{\Delta t}{\Delta x}\right)=C_{r,s}^{m}+\frac{\Delta t}{\Delta x}C_{r-1,s}^{m+1}+\frac{a\Delta t}{(\Delta y)^2}\left(C_{r-1,s+1}^{m}-2C_{r-1,s}^{m}+C_{r-1,s-1}^{m}\right) \tag{36}$$

This numerical scheme is explicit like eq. (33). However, its stability criteria are different, as shown in the Appendix. The criteria for stability of the numerical scheme of eq. (36) are

$$\left[\frac{2a\Delta x}{(\Delta y)^2},\ \frac{2a\Delta t}{(\Delta y)^2}\right]\le 1 \tag{37}$$

When steady state conditions are established, we apply the relationship of eq. (25) to obtain from eq. (36)

$$C_{r,s}=C_{r-1,s}+\frac{a\Delta x}{(\Delta y)^2}\left(C_{r-1,s+1}-2C_{r-1,s}+C_{r-1,s-1}\right) \tag{38}$$

Eq. (38) represents the explicit numerical scheme for the solution of the parabolic differential equation given by eq. (30). This scheme is subject to the stability criterion

$$\frac{2a\Delta x}{(\Delta y)^2}\le 1 \tag{39}$$

The linear combination of eqs. (35) and (38) produces the unconditionally stable scheme of Crank-Nicolson

$$\begin{aligned}&-\frac{a\Delta x}{2(\Delta y)^2}C_{r,s-1}+\left[1+\frac{a\Delta x}{(\Delta y)^2}\right]C_{r,s}-\frac{a\Delta x}{2(\Delta y)^2}C_{r,s+1}\\&=\frac{a\Delta x}{2(\Delta y)^2}C_{r-1,s-1}+\left[1-\frac{a\Delta x}{(\Delta y)^2}\right]C_{r-1,s}+\frac{a\Delta x}{2(\Delta y)^2}C_{r-1,s+1}\end{aligned} \tag{40}$$

Although the possible presentation of the finite difference approximations of eqs. (35), (38) and (40) is well known and documented, we find it appropriate to compare the performance of these schemes for the simulation of the establishment of the ROI in domains like the one of fig. 1. In fig. 7 the numerical results obtained by use of eqs. (35), (38) and (40) are compared with the analytical solution of eq. (31).

The numerical scheme solution of eq. (33) converges to the steady state solution of eq. (35) when $t > x_{max}$.

The numerical solution of eq. (36) converges to the steady state solution of eq. (38) when $t > x_{max}$.

Figure 7 indicates that the numerical results obtained by the explicit schemes of eqs. (36) and (38) provide better fit to the analytical solution than the explicit scheme of eq. (33) and implicit scheme of eq. (35). Values of δ according to eq. (38) are smaller than those given by eq. (35), as values of $\partial^2 C/\partial y^2$ are larger at $x + \Delta x$ than at x.

In fig. 8 we compare the development of δ obtained by eq. (19) with the development of that parameter according to eq. (36). We also introduce the steady state value of δ obtained by eq. (31). Fig. 8 shows minor differences in values of δ obtained by the different solutions. However, eq. (19) implies a larger time period for the build-up of the ROI, than implied by eq. (36). According to eq. (36) steady state, conditions are established and the build-up of the ROI is completed at $t \approx x_{max}$. According to eq. (19) the ROI build-up is completed at $t = 2x_{max}$. However, in the second half of that time period, changes in values of δ, according to eq. (19) are very minor.

The Boundary Layer (BL) Approximation

It is shown in the preceding section that the numerical solution of eq. (29) provides a practical and acceptable approximation for the description of the build-up of the ROI. However, some more and simpler approximations can be useful as shown hereafter.

The classical boundary layer (CBL) approximation has been used as a method for the solution of partial differential equations by von-Karman and Pohlhausen (Schlichting, 1958). They have applied this method to phenomena of fluid flow. Since then the method has been used in a variety of topics associated with fluid flows, heat transfer and mass transfer (Ozisik, 1980). The application of the CBL method to the calculation of transport phenomena is groundwater has been demonstrated in numerous publications (e.g. Wooding, 1963, 1964 and 1971; Dagan, 1971;

Eldor and Dagan, 1972; Gelhar and Collins, 1971). Various studies (e.g. Rubin and Pinder, 1979; Rubin, 1983; Rubin and Pistiner, 1986; McElwee and Kemblowski, 1990) have employed the CBL approach to analyze mineralization processes in groundwater.

Recent study of the author (Rubin, 1994) shows that the CBL method can greatly be improved by specifying the value of the contaminant concentration at the top of the BL. Therefore, the method is termed as the top specified BL (TSBL) approximation. According to this method the ROI is defined as part of the domain in which the contaminant concentration exceeds an acceptable defined value C_T. The ROI is considered as a BL, and at $y = \delta$ the contaminant concentration is $C = C_T$. The value of δ is given as

$$\delta = \delta(x,t) \tag{41}$$

From practical view point we assume that contaminant concentration vanishes where the contaminant concentration is lower by at least an order of magnitude than the acceptable level. The contaminant concentration practically goes to zero at $y = \delta_0$ where

$$\delta_0 = \delta_0(x,t);\ \ \delta_0 > \delta \tag{42}$$

We assume that in the contaminated region, which is larger than the ROI

$$C = C_b L(\eta);\ \ \eta = y/\delta_0 \tag{43}$$

where C_b is the value of C at $y = 0$.

The ROI is extended between $y = 0$ and $y = \delta$. The ordinate $y = \delta$ is termed as the top of the BL which represents the boundary of the ROI. At that location

$$y = \delta;\ \ \eta = \eta_T = \delta/\delta_0;\ \ C = C_T = C_b L(\eta_T) \tag{44}$$

We integrate eq. (29) along the vertical y coordinate between $y = 0$ and $y = \delta_0$ and use Leibniz's theorem to obtain

$$\frac{\partial}{\partial t}\left(\int_0^{\delta_0} C dy\right) + \frac{\partial}{\partial x}\left(\int_0^{\delta_0} C dy\right) = -a\left[\frac{\partial C}{\partial y}\right]_{y=0} \tag{45}$$

The value of $L(\eta)$ should be (Rubin, 1994)

$$L(\eta) = (1-\eta)^n \tag{46}$$

where n is a power coefficient determined by the best fit of the concentration profile represented by eq. (43) to measured values of C.

Introducing eqs. (43) and (46) into eq. (45) we obtain

$$\frac{\partial}{\partial t}(\delta_0 C_b)+\frac{\partial}{\partial x}(\delta_0 C_b)=an(n+1)C_b/\delta_0 \tag{47}$$

According to eqs. (44) and (46)

$$\frac{\delta}{\delta_0}=1-\left(\frac{C_T}{C_b}\right)^{\frac{1}{n}} \tag{48}$$

If the contaminant concentration is prescribed at $y = 0$, then eq. (9) implies

$$C_b=1 \tag{49}$$

If the contaminant mass flux is prescribed at y = 0, then eqs. (10), (43) and (46) imply

$$C_b=\frac{q_R\delta_0}{an} \tag{50}$$

Introduction of either one of eqs. (49) or (50) into eq. (47) yields

$$\frac{\partial}{\partial t}(\delta_0^2)+\frac{\partial}{\partial x}(\delta_0^2)=A \tag{51}$$

where

$$A=2an(n+1) \quad \textit{if } C \textit{ is prescribed at } y=0 \tag{52}$$

$$A=an(n+1) \quad \textit{if } q_R \textit{ is prescribed at } y=0 \tag{53}$$

If C is specified at $y = 0$, then we introduce eq. (49) into eq. (48) to obtain

$$\delta=\delta_0\left[1-C_T^{\frac{1}{n}}\right] \tag{54}$$

If q_R is specified at $y = 0$, then we introduce eq. (50) into eq. (48) to obtain

$$\delta=\delta_0\left[1-\left(\frac{C_T an}{q_R\delta_0}\right)^{\frac{1}{n}}\right] \tag{55}$$

Equation (51) is subject to the initial and boundary conditions

$$\delta_0=\delta_0(x,t)$$

$$\delta_0(x,0)=0$$

$$\delta_0(0,t)=0 \tag{56}$$

Equation (51) subject to the initial and boundary conditions of eq. (56) can easily be solved by the Laplace transform method to obtain

$$\delta_0^2 = A[t-(t-x)u(t-x)] \tag{57}$$

where

$$u(t-x)=\begin{cases}1 & if\ t>x\\ 0 & if\ t<x\end{cases} \tag{58}$$

According to eq. (57) steady state conditions are established in the domain when $t = x_{max}$. Eqs. (52)–(58) provide analytical expressions for δ and δ_0. However, we find it appropriate also to consider the numerical solution of eq. (51), as the basic features of this equation are not changed if some non-uniformity is introduced into the domain of fig. 1. But the non-uniformity of the domain may avoid the availability of a simple analytical solution of eq. (51). Then numerical procedure should be used.

Equation (51) is a first order hyperbolic equation in the x, t plane. We adopt the explicit-implicit approach for the solution of this equation by finite difference approximation. By such an approach eq. (51) yields

$$\frac{\left(\delta_0^2\right)_r^{m+1}-\left(\delta_0^2\right)_r^m}{\Delta t}+\frac{\left(\delta_0^2\right)_r^{m+1}-\left(\delta_0^2\right)_{r-1}^{m+1}}{\Delta x}=A \tag{59}$$

This expression yields the following explicit numerical scheme

$$\left(\delta_0^2\right)_r^{m+1}\left[1+\frac{\Delta t}{\Delta x}\right]=\left(\delta_0^2\right)_r^m+\frac{\Delta t}{\Delta x}\left(\delta_0^2\right)_{r-1}^{m+1}+A \tag{60}$$

This numerical scheme is unconditionally stable.

In fig. 9 we compare the steady state values of δ, when $C = 1$ is prescribed at $y = 0$, according to eqs. (27), (31) and (57). The chosen value of $n = 3$, as suggested by Rubin (1994) seems to be quite appropriate for the employment of the TSBL approximation. Some other tests of the analytical solution of the TSBL approach have been performed by Rubin (1994). They indicated that the TSBL provided very good approximation to the various solutions, with smaller amount of approximation, of the diffusion-advection equation. We find it appropriate to compare the analytical solution of eq. (57) with the numerical solution of eq. (60).

In fig. 10 we compare the development of δ, in a domain subject to contamination due to prescribed C value at $y = 0$, as implied by eqs. (57) and (60). This figure indicates that the numerical scheme of eq. (60) converges quite well to the analytical steady state solution. Differences in intermediate states are minor. However, the build-up of the ROI is completed, according to eq. (60) in a time period longer than x_{max}.

Discussion

This report concerns some possible approximate approaches that can be useful in initial stages of evaluation and analysis of groundwater contamination. We introduce a simplified conceptual model of an aquifer subject to contamination and present a hierarchy of approximation methods that can be useful in the process of the evaluation of the contaminant transport in the groundwater system. Due to the uniformity of the domain shown in fig. 1, dimensionless variables could be used and all types of approximate methods could be employed.

It is indicated that whenever all types of approximation can be used, differences between the various types of numerical solution results are very minor. However, the more complex the domain, the smaller the amount of approximation that can be introduced into the basic flow and transport equations. The higher the approximation that can be introduced into the system of the basic equations, the simpler is the numerical solution, stability criteria are less restrictive, and sometimes analytical solutions can be found. The largest amount of approximation is introduced when using the BL approach.

The applicability of the BL method is the most restrictive from the point of view of non-uniformity that can be considered in the aquifer. However, the TSBL method can also be applied in a variety of non-uniformities. Therefore, we have considered uses of a numerical scheme for this method even though the TSBL approach leads to analytical solutions when contaminant transport in the domain of fig. 1 is evaluated.

It is suggested that initial evaluation of groundwater contamination would be done by use of the simplified approaches and numerical schemes presented in this document. The basic

schemes of this document can easily be extended to some more complicated systems than the one shown in fig. 1. The initial evaluation by use of the approximate schemes can save much effort needed to make the numerical calculations by using extremely sophisticated "black box models."

Summary

A hierarchy of approximate approaches applicable for the simulation of groundwater contamination is presented. First stage of approximation is introduced by adopting the Dupuit approximation to an extremely simplified conceptual model of the aquifer. Then the equation of diffusion-advection collapses to a differential equation incorporating a single advection term. As advection is much more significant than diffusion in the direction of the flow in the domain, the second stage of approximation is invited, in which longitudinal dispersion is neglected. Under such conditions the large extent of the domain and uniformity of the aquifer in the vertical direction invite using the BL approximation. We prefer to employ the TSBL approach due to its higher reliability and broader scope of applications.

Each approximate method usage is exemplified by the development of appropriate finite difference numerical schemes. The stability of each scheme is evaluated and analyzed. In such a manner a complete information regarding the advantages of the various types of approximate methods is given. The reliability of the different types of approximation and numerical schemes has been evaluated by comparing results of the various types of approximation with solutions with smaller amount of approximation, or whenever possible comparing the numerical results with analytical solutions.

Appendix: Stability Analysis

Stability of Eq. (17)

We employ the procedure of von-Neumann (e.g. Lapidus and Pinder, 1982) in order to analyze the stability of the numerical scheme given by eq. (17).

We introduce an initial line of error which is represented by a finite Fourier series as follows:

$$C_{r,s}^{m} = e^{\gamma m\Delta t} e^{i\beta_1 r\Delta x} e^{i\beta_2 s\Delta y} \tag{A1}$$

We define the amplification factor ξ as

$$\xi = e^{\gamma\Delta t} \tag{A2}$$

Introducing eqs. (A1) and (A2) into eq. (17) we obtain

$$\xi\left[1+\frac{\Delta t}{\Delta x}\left(1-e^{-i\beta_1\Delta x}\right)\right] = 1+\frac{a_L\Delta t}{(\Delta x)^2}\left(e^{i\beta_1\Delta x}-2+e^{-i\beta_1\Delta x}\right)+\frac{a\Delta t}{(\Delta y)^2}\left(e^{i\beta_2\Delta y}-2+e^{-i\beta_2\Delta y}\right) \tag{A3}$$

We employ the following relationships

$$\begin{aligned} e^{i\beta h}+e^{-i\beta h} &= 2\ \cos\ \beta h \\ e^{i\beta h}-e^{-i\beta h} &= 2i\ \sin\ \beta h \end{aligned} \tag{A4}$$

where β is a dummy variable representing β_1 or β_2, and h is a dummy variable representing Δx or Δy.

Introducing eq. (A4) into eq. (A3) we obtain

$$\xi = \frac{1+\frac{2a_L\Delta t}{(\Delta x)^2}\left(\cos\ \beta_1\Delta x-1\right)+\frac{2a\Delta t}{(\Delta y)^2}\left(\cos\ \beta_2\Delta y-1\right)}{1+\frac{\Delta t}{\Delta x}\left(1-\cos\ \beta_1\Delta x+i\ \sin\ \beta_1\Delta x\right)} \tag{A5}$$

The numerical scheme of eq. (17) is stable provided that

$$|\xi| \le 1 \tag{A6}$$

Equations (A5) and (A6) should yield the criteria for stability of eq. (17) when extreme cases are considered. We consider

$$\cos\ \beta_1\Delta x = \cos\ \beta_2\Delta y = -1 \tag{A7}$$

Introducing eq. (A7) into eq. (A5), the following stability criterion is obtained

$$\frac{2a_L\Delta t}{(\Delta x)^2}+\frac{2a\Delta t}{(\Delta y)^2} \le 1+\frac{\Delta t}{\Delta x} \tag{A8}$$

Consider

$$\cos\ \beta_1\Delta x = 1;\ \cos\ \beta_2\Delta y = -1 \tag{A9}$$

Introducing eq. (A9) into eq. (A5), the following stability criterion is obtained

$$\frac{2a\Delta t}{(\Delta y)^2} \le 1 \tag{A10}$$

Both criteria represented by eqs. (A8) and (A10) should be satisfied in order that eq. (17) may represent a stable numerical scheme.

Stability of eq. (19)

We introduce the line of error represented by eqs. (A1) and (A2) into eq. (19) and obtain

$$\xi\left[1+\frac{\Delta t}{\Delta x}\left(1-e^{-i\beta_1\Delta x}\right)\right] = 1+\frac{a_L\Delta t}{(\Delta x)^2}\left(e^{i\beta_1\Delta x}-2+e^{-i\beta_1\Delta x}\right) + \frac{a\Delta t}{(\Delta y)^2}\left(e^{-i\beta_1\Delta x}\right)\left(e^{i\beta_2\Delta y}-2+e^{-i\beta_2\Delta y}\right) \tag{A11}$$

Introducing eq. (A4) into eq. (A11) we obtain

$$\xi = \frac{1+\frac{2a_L\Delta t}{(\Delta x)^2}(\cos\ \beta_1\Delta x-1)+\frac{2a\Delta t}{(\Delta y)^2}(\cos\ \beta_1\Delta x-i\ \sin\ \beta_1\Delta x)(\cos\ \beta_2\Delta y-1)}{1+\frac{\Delta t}{\Delta x}(1-\cos\ \beta_1\Delta x+i\ \sin\ \beta_1\Delta x)} \tag{A12}$$

The numerical scheme of eq. (19) is stable provided that eq. (A6) is satisfied. Several extreme cases should be analyzed.

Considering the relationships represented by eq. (A7) we obtain

$$\frac{2a\Delta x}{(\Delta y)^2}-\frac{2a_L}{\Delta x} \le 1 \tag{A13}$$

$$\frac{2a_L\Delta t}{(\Delta x)^2}-\frac{2a\Delta t}{(\Delta y)^2} \le 1+\frac{\Delta t}{\Delta x} \tag{A14}$$

Considering the relationships given by eq. (A9), the stability criterion represented by eq. (A10) is obtained.

Stability of eq. (33)

We introduce the line error represented by eqs. (A1) and (A2) into eq. (33) and obtain

$$\xi\left[1+\frac{\Delta t}{\Delta x}\left(1-e^{-i\beta_1\Delta x}\right)\right] = 1+\frac{a\Delta t}{(\Delta y)^2}\left(e^{i\beta_2\Delta y}-2+e^{-i\beta_2\Delta y}\right) \tag{A15}$$

Introducing eq. (A4) into eq. (A15) we obtain

$$\xi = \frac{1 + \frac{2a\Delta t}{(\Delta y)^2}(\cos\ \beta_2 \Delta y - 1)}{1 + \frac{\Delta t}{\Delta x}(1 - \cos\ \beta_1 \Delta x + i\ \sin\ \beta_1 \Delta x)} \tag{A16}$$

The numerical scheme of eq. (33) is stable provided that eq. (A6) is satisfied. The extreme case is represented by eq. (A9). It yields the stability criterion given by eq. (A10).

Stability of eq. (36)

We introduce the line error represented by eqs. (A1) and (A2) into eq. (36) and obtain

$$\xi\left[1 + \frac{\Delta t}{\Delta x}\left(1 - e^{-i\beta_1 \Delta x}\right)\right] = 1 + \frac{a\Delta t}{(\Delta y)^2}\left(e^{-i\beta_1 \Delta x}\right)\left(e^{i\beta_2 \Delta y} - 2 + e^{-i\beta_2 \Delta y}\right) \tag{A17}$$

Introducing eq. (A4) into eq. (A17) we obtain

$$\xi = \frac{1 + \frac{2a\Delta t}{(\Delta y)^2}(\cos\ \beta_1 \Delta x - i\ \sin\ \beta_1 \Delta x)(\cos\ \beta_2 \Delta y - 1)}{1 + \frac{\Delta t}{\Delta x}(1 - \cos\ \beta_1 \Delta x + i\ \sin\ \beta_1 \Delta x)} \tag{A18}$$

The numerical scheme of eq. (36) is stable provided that eq. (A6) is satisfied. Several extreme cases should be analyzed.

Considering the relationships represented by eq. (A7) we obtain

$$\frac{2a\Delta x}{(\Delta y)^2} \leq 1 \tag{A19}$$

Considering the relationships represented by eq. (A9) the criterion given by eq. (A10) is obtained.

References

Carslaw, H.S. and Jaeger, J.C., 1959. "Conduction of Heat in Solids," 2nd ed., Oxford at the Clarendon Press, London, U.K., p. 63, 75.

Dagen, G., 1971. Perturbation solutions of the dispersion equation in porous mediums, Water Resource Research, 7:135.

Eldor, M. and Dagen, G., 1972. Solutions of hydrodynamic dispersion in porous media, Water Resources Research, 8:1316

Gelhar, L.W. and Collins, M.A., 1971. General analysis of longitudinal dispersion in nonuniform flow, Water Resources Research, 7:1511.

Hunt, B., 1978. Dispersion calculations in nonuniform seepage, Journal of Hydrology, 36:261.

Lapidus, L. and Pinder, G.F., 1982. "Numerical Solution of Partial Differential Equations in Science and Engineering," John Wiley & Sons, New York.

McElwee, C. and Kemblowski, M., 1990. Theory and application of an approximate model of saltwater upconing in aquifers, Journal of Hydrology, 115:139–163.

Ozisik, M.N., 1980. "Heat Conduction," Wiley-Interscience, New York, p. 335.

Rubin, H., 1983. On the application of the boundary layer approximation for the simulation of density stratified flows in aquifers, Advances in Water Resources, 6:96–105.

Rubin, H., 1994. Approximate methods for the simulation of groundwater contamination processes, Open-File Report 94-8, Kansas Geological Survey, the University of Kansas; Lawrence, Kansas.

Rubin, H. and Pinder, G.F., 1977. Approximate analysis of upconing, Advances in Water Resources, 1:97–101.

Rubin, H. and Pistiner, A., 1986. Modelling fresh water injection into a partially saline partially fresh (PASPAF) aquifer, Journal of Hydrology, 37:351–378.

Schliching, H., 1988. "Boundary layer Theory," 6th ed., McGraw-Hill, New York, p. 335.

Wooding, R.A., 1963. Convection in a saturated porous medium at large Rayleigh number or Péclet number, Journal of Fluid Mechanics, 15:527.

Wooding, R.A., 1964. Mixing layer flows in a saturated porous medium, Journal of Fluid Mechanics, 19:103.

Wooding, R.A., 1971. Groundwater problems of the interaction of saline and freshwater, in "Salinity and Water Use," Talsma, T. and Philip, J.R. (eds.), Wiley-Interscience, New York, p. 125.

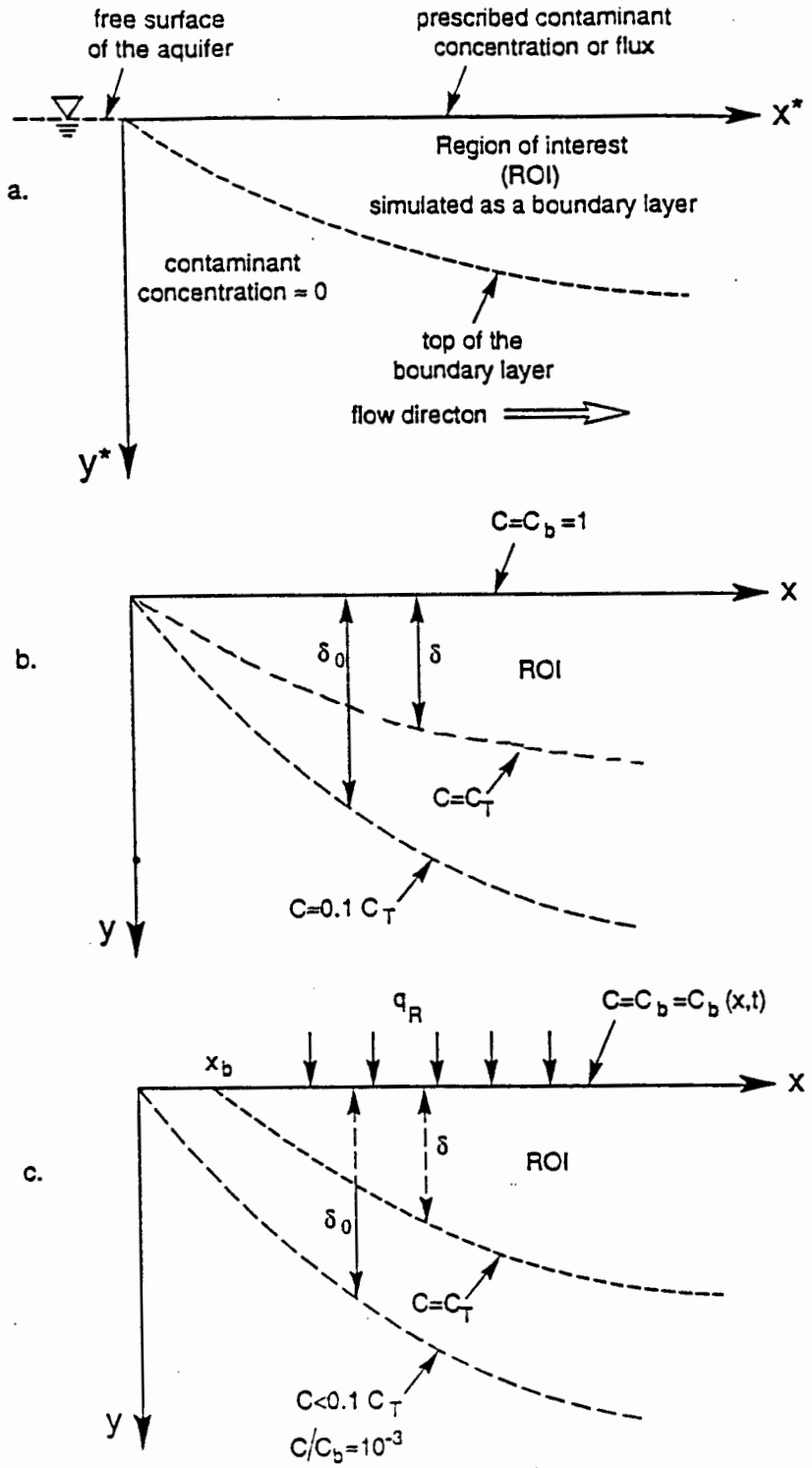

Fig. 1 The conceptual model of the aquifer subject to contamination

(a) Regions of classification

(b) Definition of dimensionless quantities when contaminant concentration is prescribed at $y = 0$

(c) Definition of dimensionless quantities when contaminant flux is prescribed at $y = 0$

Fig. 2 Development of δ according to eqs. (17), (19) and (27), ($a = 0.5$; $a_L = 5$; $\Delta x = \Delta y = 1$; $\Delta t = 0.1$)

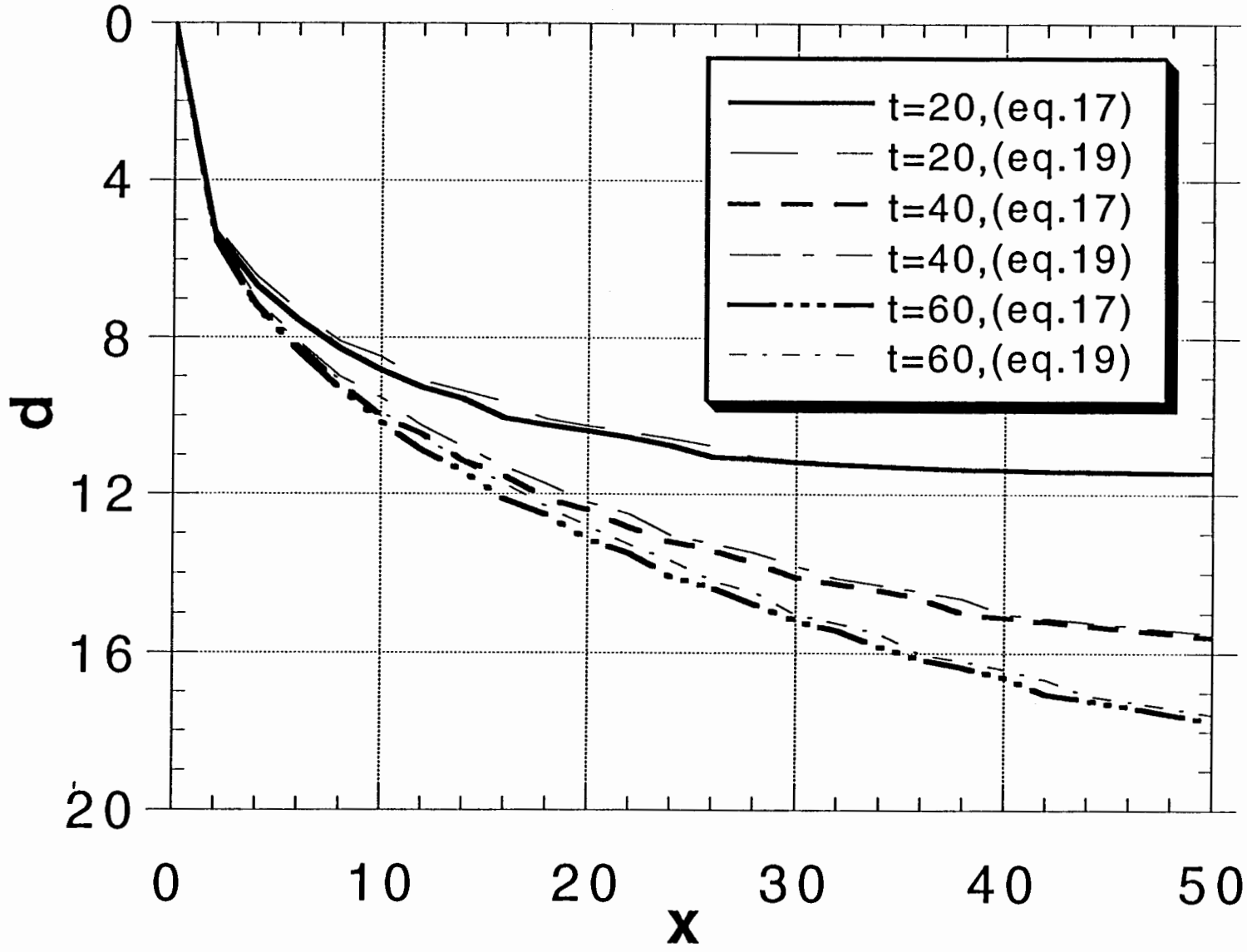

Fig. 3 Steady state values of δ according to eqs (17), (19) and (27), ($a = 0.5$; $a_L = 5$; $\Delta x = \Delta y = 1$; $\Delta t = 0.1$)

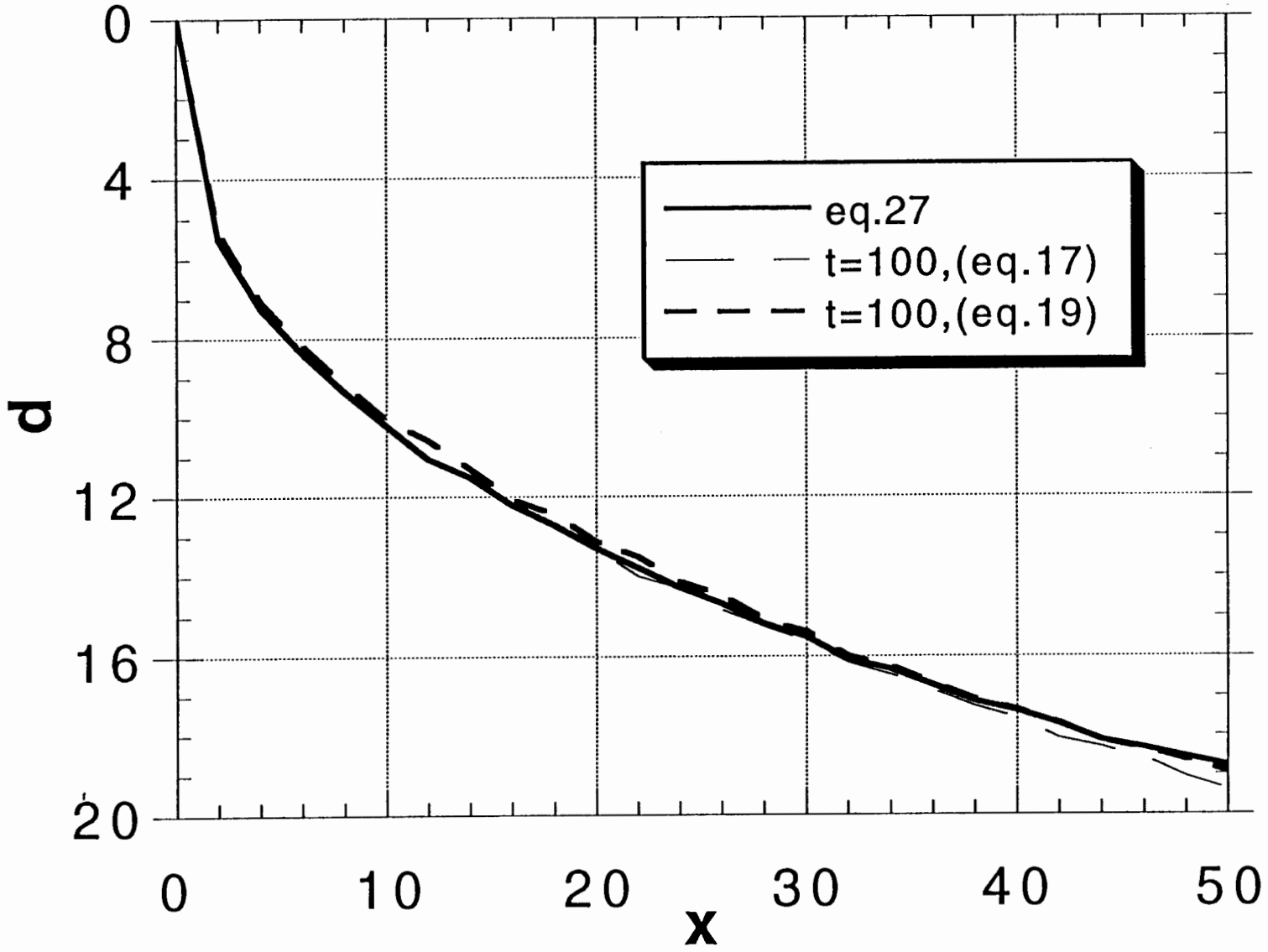

Fig. 4 Development of δ according to eq. (17), ($q_R = 0.1$; $a = 0.5$; $a_L = 5$; $\Delta x = \Delta y = 1$; $\Delta t = 0.1$)

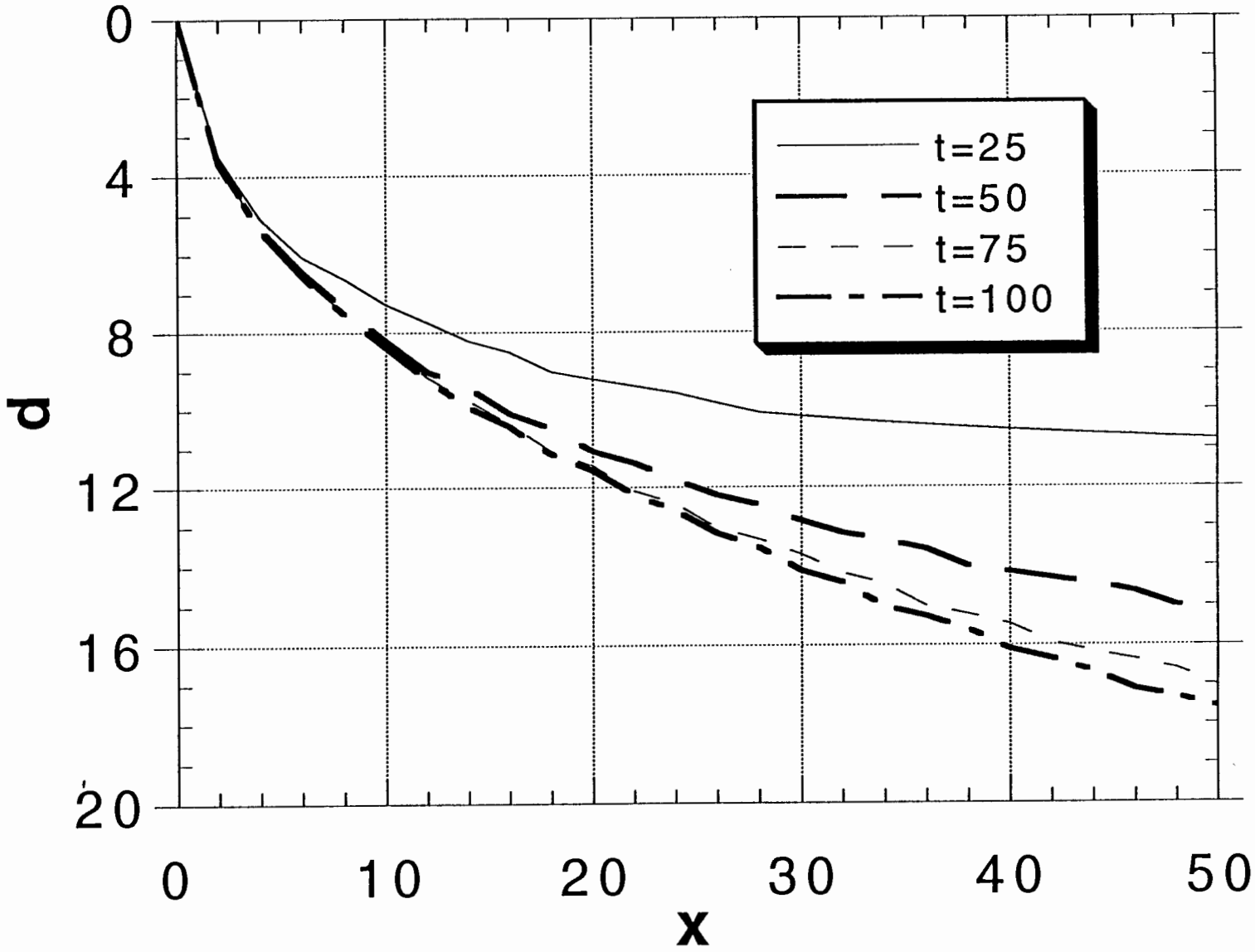

Fig. 5 Steady state values of δ according to eqs. (27) and (31),

($a = 0.05, 0.1, 0.5$; $\Delta x = \Delta y = 1.0$)

(a) $a_L = 0.5$

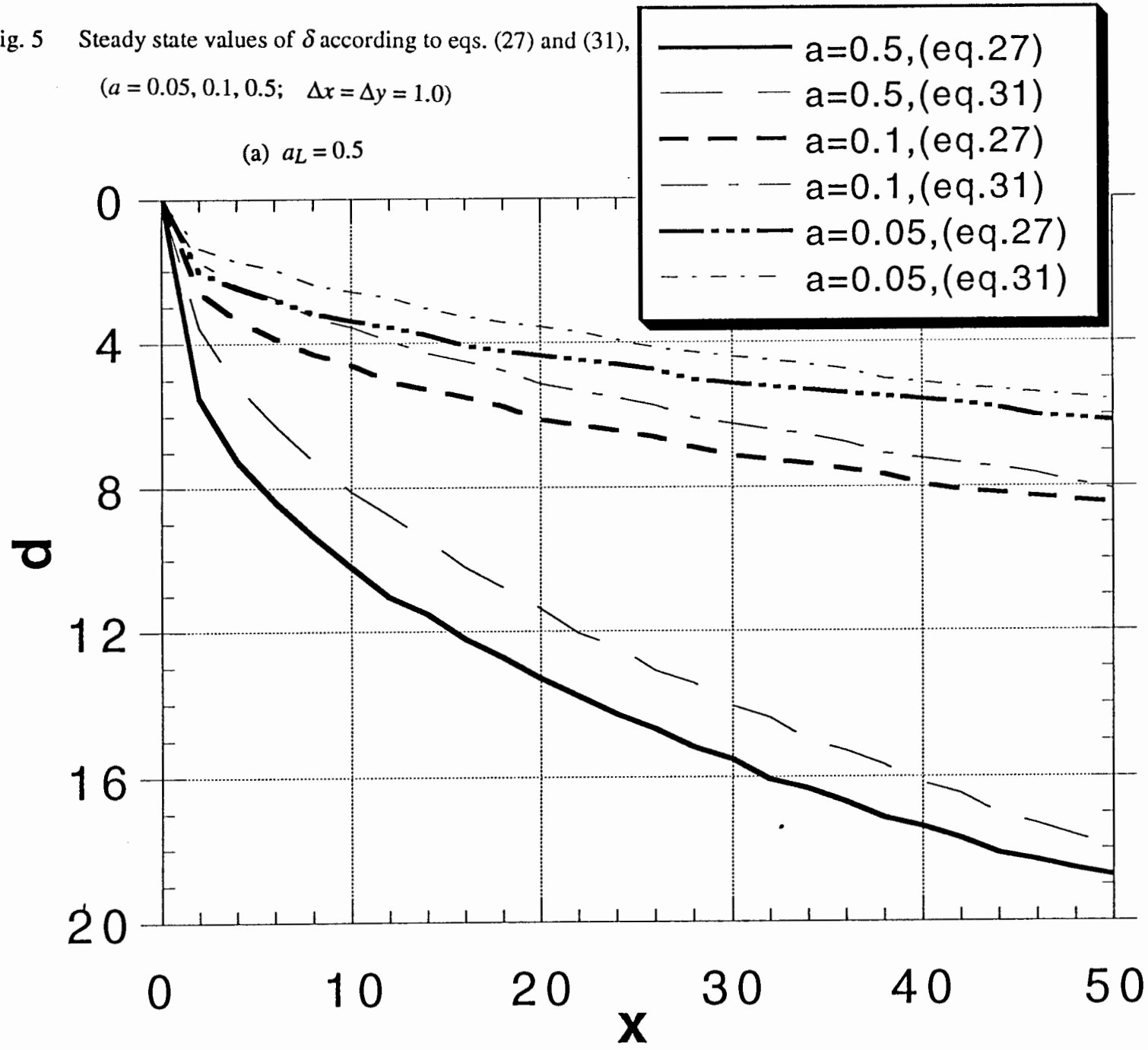

Fig. 5 Steady state values of δ according to eqs. (27) and (31), (a = 0.05, 0.1, 0.5; $\Delta x = \Delta y = 1.0$)

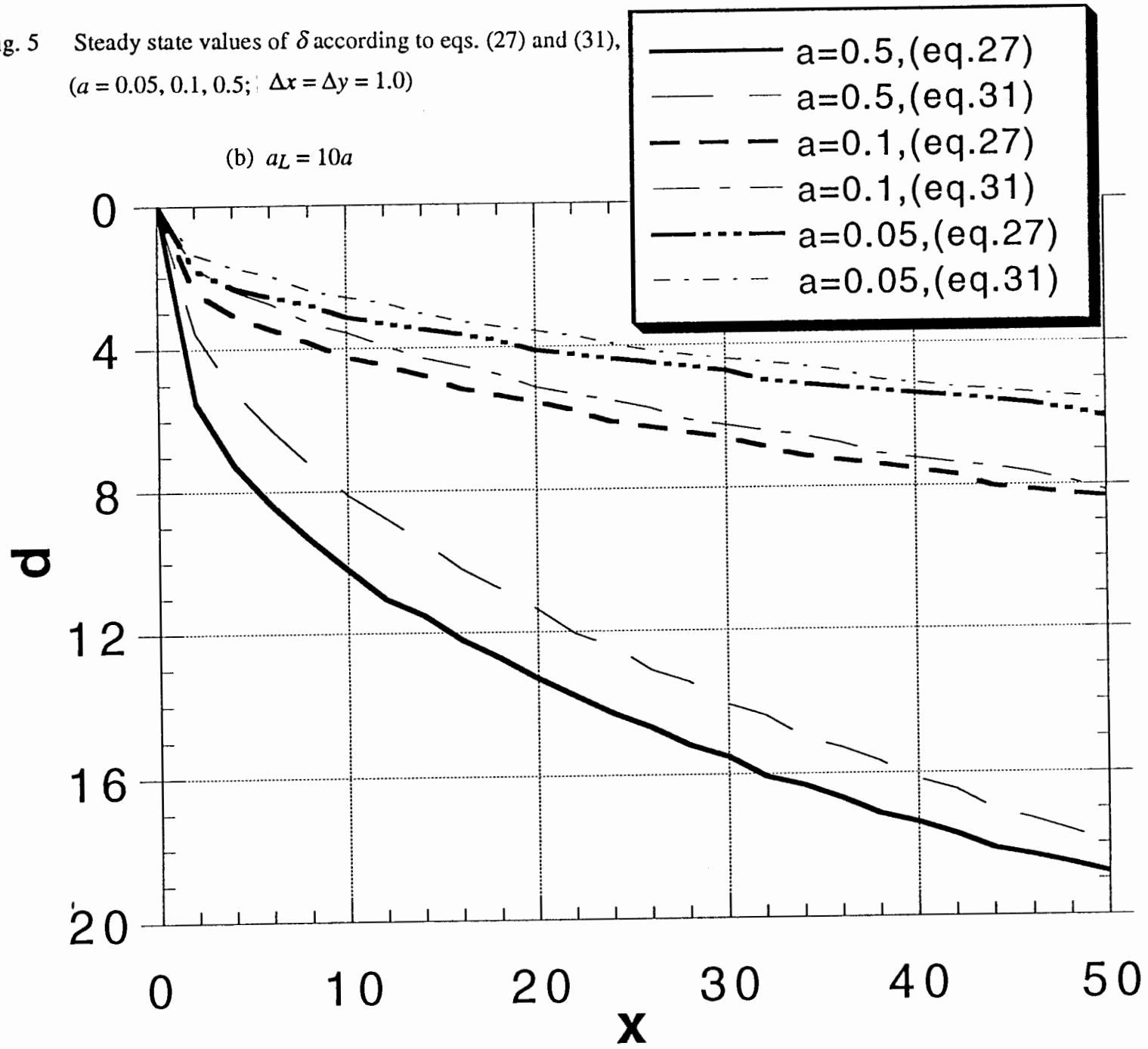

Fig. 6 Steady state contaminant concentration profiles according to eqs. (27) and (31) ($a = 0.5$, $a_L = 5$; $\Delta x = \Delta y = 1.0$)

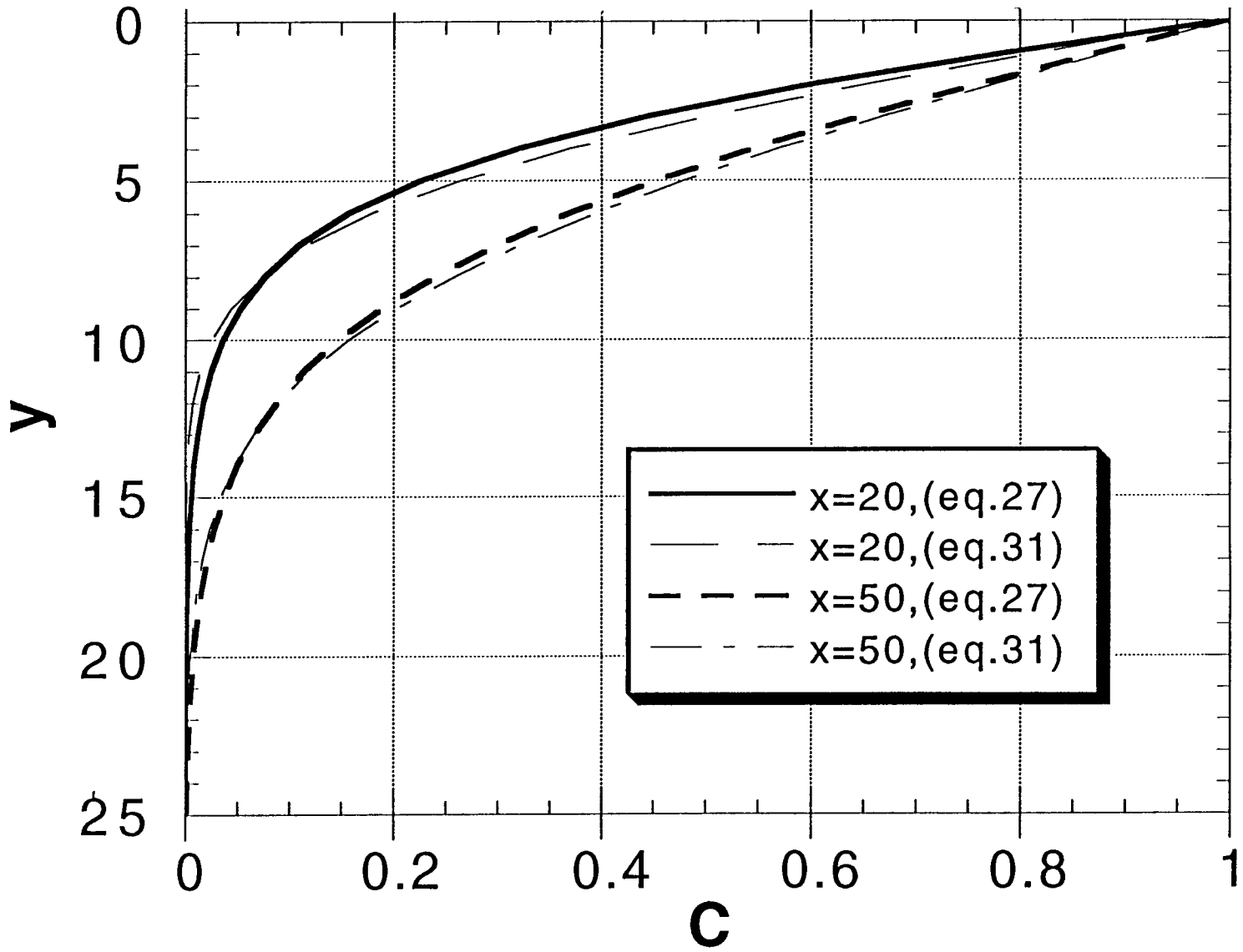

Fig. 7 Steady state values of δ according to eqs. (31), (35), (38) and (40) ($a = 0.5$; $\Delta x = \Delta y = 1.0$)

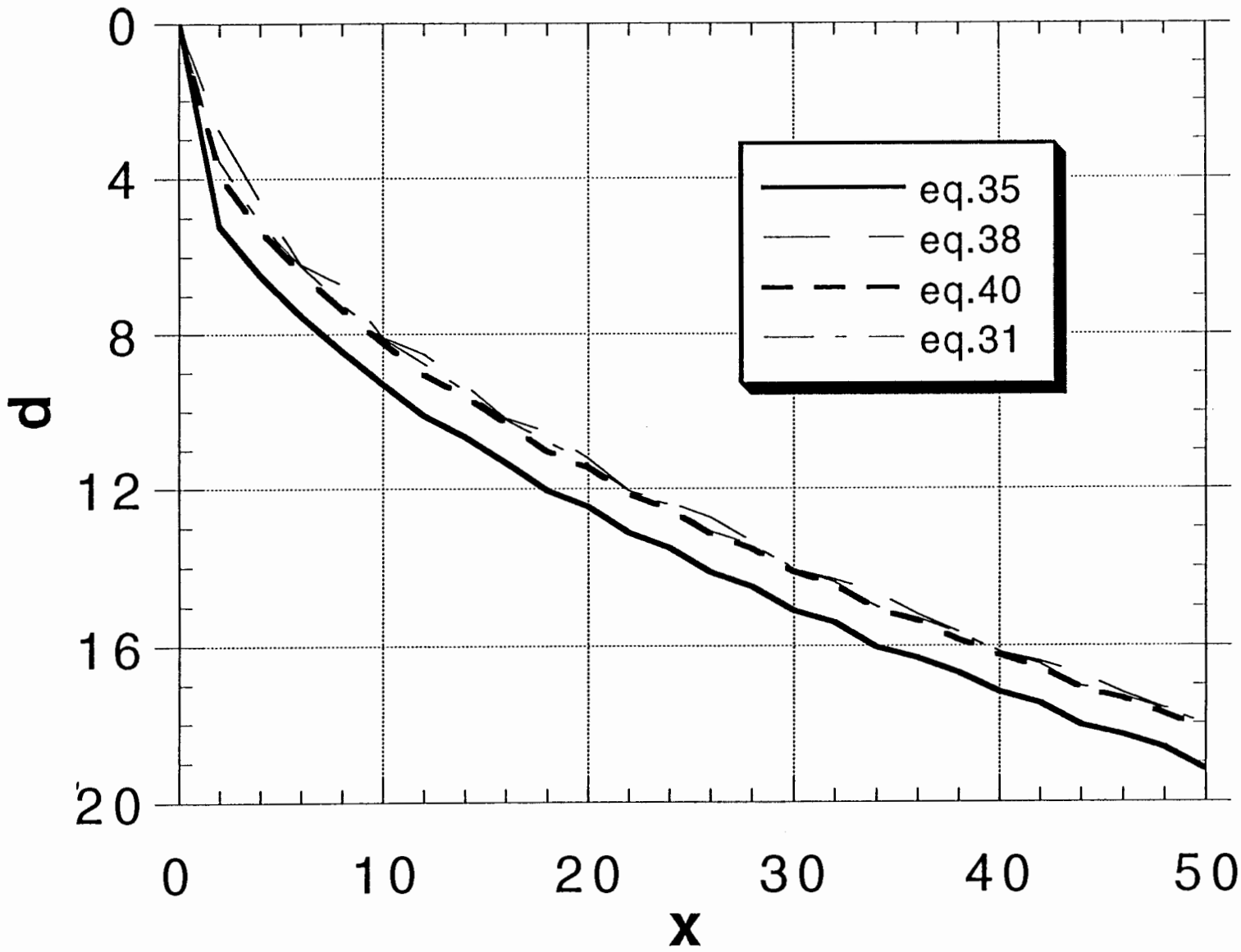

Fig. 8 Development of δ according to eqs. (19), (36) and (31), ($a = 0.5$; $a_L = 5$)

In eq. (19) $\Delta x = \Delta y = 1.0$; $\Delta t = 0.1$

In eq. (36) $\Delta x = \Delta y = \Delta t = 1.0$

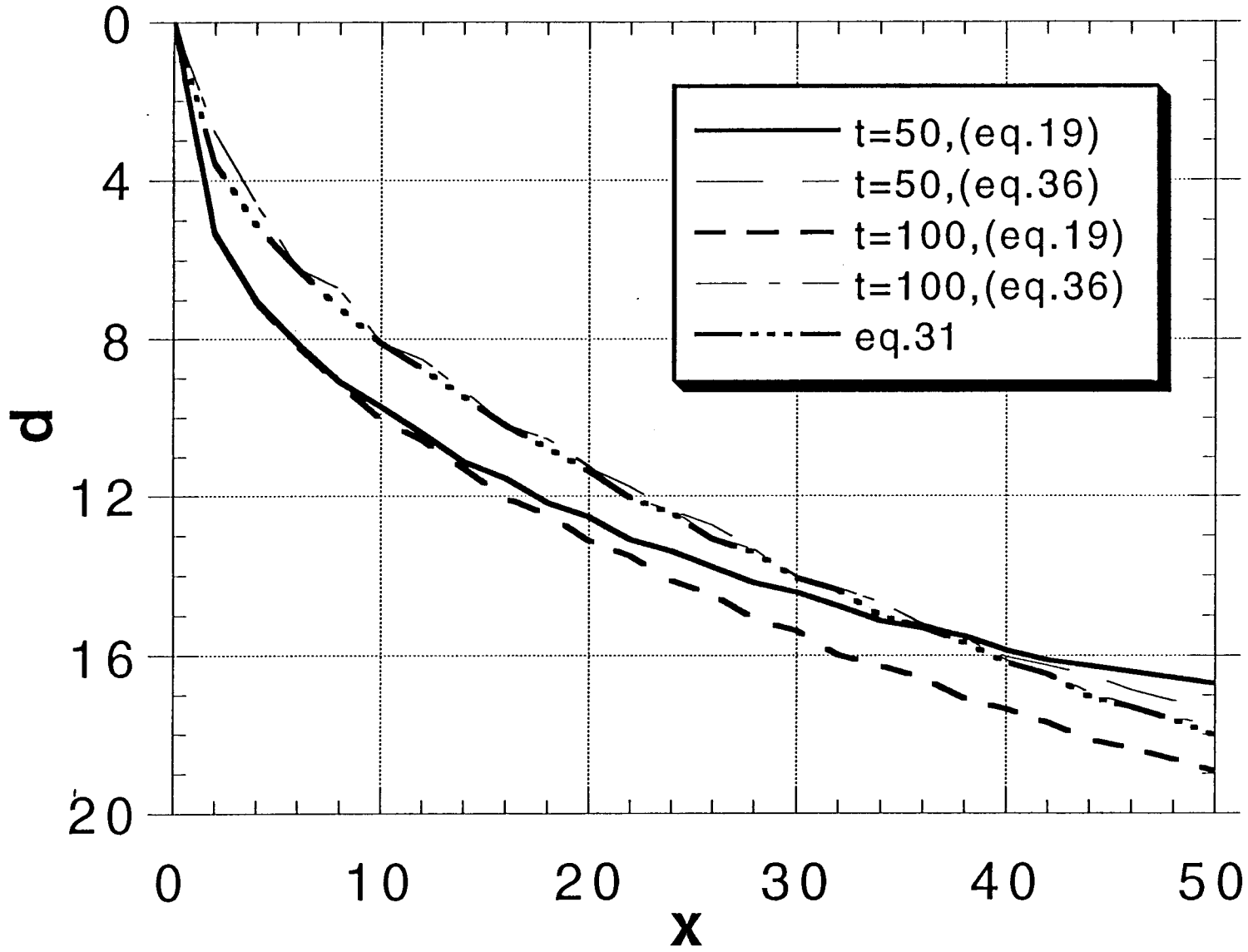

Fig. 9 Steady state values of δ according to eqs. (27), (31) and (57), ($a = 0.5$; $a_L = 5$; $n = 3$; $\Delta x = \Delta y = 1.0$)

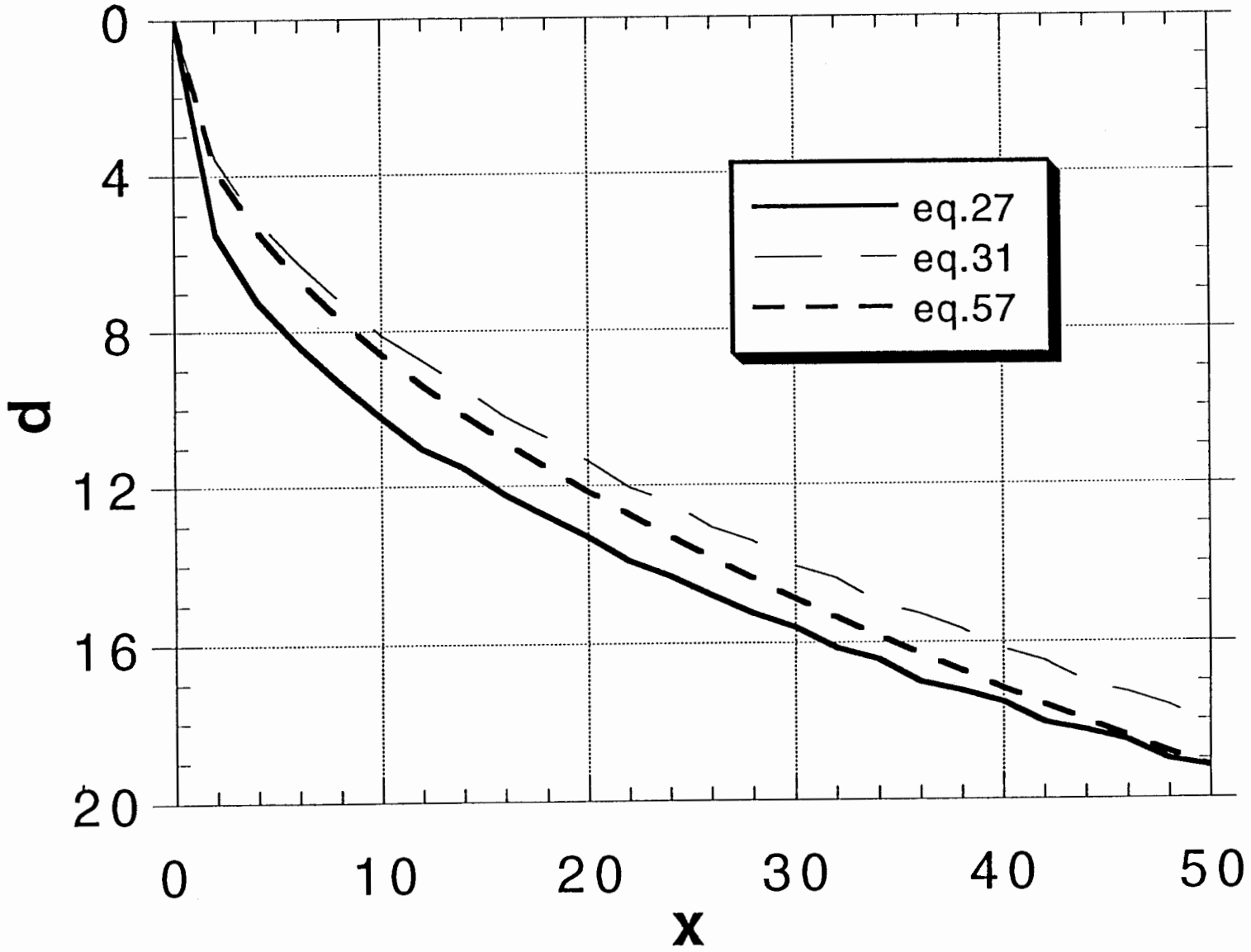

Fig. 10 Development of δ according to eqs. (57) and (60), ($a = 0.5$; $n = 3$; $\Delta x = \Delta y = 1.0$)